The Journal of Chemical Physics

Isotopomer-selective spectra of a single *intact* H_2O molecule in the $Cs^+(D_2O)_5H_2O$ isotopologue: Going beyond pattern recognition to harvest the structural information encoded in vibrational spectra

Cite as: J. Chem. Phys. **144**, 074305 (2016); https://doi.org/10.1063/1.4941285
Submitted: 16 November 2015 . Accepted: 21 January 2016 . Published Online: 17 February 2016

Conrad T. Wolke, Joseph A. Fournier, Evangelos Miliordos, Shawn M. Kathmann, Sotiris S. Xantheas, and Mark A. Johnson

Isotopomer-selective spectra of a single *intact* H_2O molecule in the $Cs^+(D_2O)_5H_2O$ isotopologue: Going beyond pattern recognition to harvest the structural information encoded in vibrational spectra

Conrad T. Wolke,[1] Joseph A. Fournier,[1] Evangelos Miliordos,[2] Shawn M. Kathmann,[2,a)] Sotiris S. Xantheas,[2,a)] and Mark A. Johnson[1,a)]
[1]*Sterling Chemistry Laboratory, Yale University, 225 Prospect Street, New Haven, Connecticut 06520, USA*
[2]*Physical Sciences Division, Pacific Northwest National Laboratory, 902 Battelle Boulevard, P.O. Box 999, Richland, Washington 99352, USA*

(Received 16 November 2015; accepted 21 January 2016; published online 17 February 2016)

We report the vibrational signatures of a single H_2O molecule occupying distinct sites of the hydration network in the $Cs^+(H_2O)_6$ cluster. This is accomplished using isotopomer-selective IR-IR hole-burning on the $Cs^+(D_2O)_5(H_2O)$ clusters formed by gas-phase exchange of a single, intact H_2O molecule for D_2O in the $Cs^+(D_2O)_6$ ion. The OH stretching pattern of the $Cs^+(H_2O)_6$ isotopologue is accurately recovered by superposition of the isotopomer spectra, thus establishing that the H_2O incorporation is random and that the OH stretching manifold is largely due to contributions from decoupled water molecules. This behavior enables a powerful new way to extract structural information from vibrational spectra of size-selected clusters by explicitly identifying the local environments responsible for specific infrared features. The $Cs^+(H_2O)_6$ structure was unambiguously assigned to the 4.1.1 isomer (a homodromic water tetramer with two additional flanking water molecules) from the fact that its computed IR spectrum matches the observed overall pattern and recovers the embedded correlations in the two OH stretching bands of the water molecule in the $Cs^+(D_2O)_5(H_2O)$ isotopomers. The 4.1.1 isomer is the lowest in energy among other candidate networks at advanced (e.g., CCSD(T)) levels of theoretical treatment after corrections for (anharmonic) zero-point energy. With the structure in hand, we then explore the mechanical origin of the various band locations using a local electric field formalism. This approach promises to provide a transferrable scheme for the prediction of the OH stretching fundamentals displayed by water networks in close proximity to solute ions. © *2016 AIP Publishing LLC.* [http://dx.doi.org/10.1063/1.4941285]

I. INTRODUCTION

A predictive theoretical framework for the spectroscopic signatures of aqueous ions is finally coming within reach as a consequence of recent experimental advances in cluster ion spectroscopy as well as theoretical methods that treat the solute and surrounding solvent molecules in the ansatz of a supermolecule.[1–4] Because vibrational spectra of cold, composition-selected cluster ions are now routinely available,[5] the next challenge becomes how to extract unambiguous structural information from the observed patterns of vibrational fundamentals and combination bands.[6,7] Here we revisit the $Cs^+(H_2O)_n$ cluster ions, for which vibrational spectra of the Ar-tagged n = 1-5 clusters were reported by Lisy and co-workers[8–10] several years ago. In this paper, we focus on the $n = 6$ cluster and first report its experimental vibrational spectrum using D_2 tagging. We then analyze the resulting pattern using a theoretical approach that does not rely on the empirical "scaling factors" commonly used to identify cluster structures by comparison with harmonic predictions. While this approach provides less biased criteria for structure identifications, it still relies on matching the *overall* pattern in the experimental spectrum, raising the question of how one might experimentally challenge the theoretical assignment of particular bands to the OH stretching displacements of water molecules that reside in distinct sites within the H-bonded network.[11] To extract this microscopic information, we adapt an IR photochemical hole burning method that directly obtains the spectra of the bands originating from a single, intact H_2O molecule incorporated into the perdeutero cluster hydrate, $Cs^+(D_2O)_5(H_2O)$.[12] This is accomplished through isotopomer-selective, IR-IR double resonance spectroscopy.[13,14] In principle, this can be viewed as the gas-phase cluster analogue of the trace isotope method well-established in condensed-phase spectroscopy of aqueous systems.[15–21] Unlike the condensed-phase, however, cluster chemistry affords a unique opportunity to study the spectra of an intact H_2O molecule by exploiting the fact that proton scrambling processes are strongly suppressed in the case of alkali ion hydration.[22,23] This circumstance thus enables an experimental way to directly determine the *correlation* between the two OH oscillators on the same water molecule as it is locked in the various network sites. We then use this information to map the OH stretching frequencies onto the effective electric fields arising from the ion and the other water molecules.

a)Authors to whom correspondence should be addressed. Electronic addresses: shawn.kathmann@pnnl.gov; sotiris.xantheas@pnnl.gov; and mark.johnson@yale.edu.

II. EXPERIMENTAL DETAILS

The Cs^+ ions were extracted from solution by electrospray ionization of 4 mM Cs_2SO_4 in D_2O and injected into the inlet capillary of a custom mass spectrometer described previously.[5,24] After the capillary, the ions were passed through three differentially pumped stages using RF only octopole ion guides before they were accumulated in a 3D Paul trap. The trap is mounted to the second stage of a 4 K helium cryostat, and the ions were cooled to roughly 30 K[25] by a pulsed helium buffer gas containing a trace amount of D_2 and N_2.[26,27] These molecules condense onto the cold ions to generate the "tags" necessary for cryogenic ion vibrational predissociation (CIVP) spectroscopy.[5,28,29] The tagged clusters were then ejected out of the Paul trap and into the acceleration region of the tandem time of flight photodissociation mass spectrometer. By controlling the partial pressure of D_2O in the gas mixture directly surrounding the electrospray tip, the Cs^+ ions are solvated by a large number of heavy water molecules. We note that, although intramolecular H/D scrambling is ubiquitous in bulk water, the groups of Uggerud and Beyer[22,23,30–32] have established that this process is strongly suppressed in $M^+(H_2O)_n$ (M = pyridinium, alkali, and transition metal cations) clusters by noting the absence of HDO evaporation using MS-MS techniques.

To replace a D_2O molecule of the cluster ensemble with a single intact H_2O, low pressure (~1 mTorr) water vapor was leaked into the guide region of the second differentially pumped ion transport stage. Ligand exchange was carried out by adjusting the pressure in this region and monitoring the resulting time of flight mass spectrum. The mass distribution evolves with a strong preference for exchange of two hydrons, as shown in the mass spectrum displayed in Fig. 1. This indicates that the labeled clusters correspond to the $Cs^+(D_2O)_5(H_2O)$ composition, which is further supported through spectroscopic behavior in the bending region (*vide infra*, see Fig. 4(c)). The minor contribution from HDO incorporation (interlopers in Fig. 1) likely results from contamination of HDO by exchange on the walls of the inlet system. We note that the integrated intensity of the water clusters of a given size is nearly conserved upon incorporation of the heavy isotopes, indicating that the process occurs by condensation followed by evaporation with very little collisional dissociation.

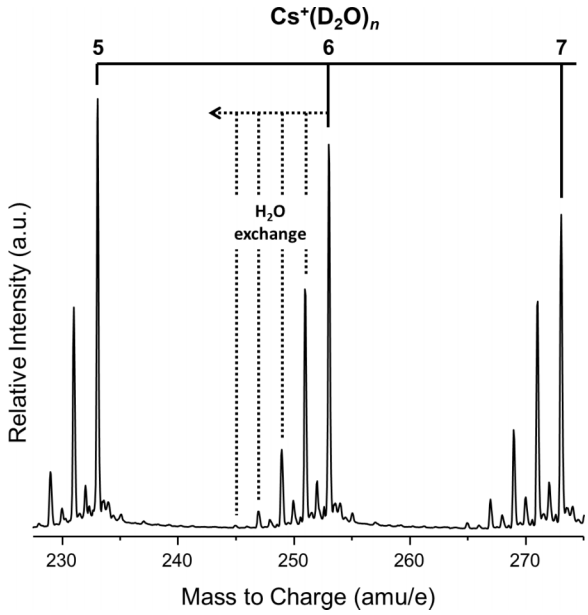

FIG. 1. Mass spectrum of the $Cs^+(D_2O)_n$ cluster distribution for $n = 5$-7. The cesium hydrate cations display a strong preference for the exchange of two hydrons (dotted lines), as expected for the substitution for an intact H_2O molecule.

The tagged $Cs^+(D_2O)_5(H_2O)$ clusters were mass-selected by a pulsed set of deflectors before the ion beam was intersected by a tunable infrared laser system (LaserVision) covering both the water bends and the OH stretches. The statistical exchange of a single H_2O molecule for D_2O results in formation of isotopomers which differ drastically in their signature OH stretch transitions according to the location of the label in the water network. These patterns were measured experimentally using IR-IR double resonance spectroscopy.[12–14]

III. RESULTS AND DISCUSSION

A. Identification of low lying isomers

Calculated structures of the hexahydrate have been reported previously at the MP2/aug-cc-pVDZ (using the effective core potential for Cs developed by Lajohn *et al.*)[8,9,33] and we begin by revisiting the search for low energy structures to establish the robustness of the energy ordering as the level of theory is increased. In particular, we performed the calculations at the MP2 level, with both the aug-cc-pVDZ and aug-cc-pVTZ basis sets for the oxygen and hydrogen centers,[34,35] and a relativistic pseudopotential combined with a triple-zeta [5s,5p,4d] uncontracted basis set for Cs (CRENBL).[36] These basis sets will be denoted as ADZ and ATZ, respectively. The 1s orbitals of all oxygen atoms were kept frozen at the MP2 level, whereas all eight semi-core *sp* atomic orbitals for Cs (5s5p) were correlated. Geometry optimizations were carried out with the NWChem suite of electronic structure codes.[37]

This procedure generated the six isomers displayed in Fig. 2, of which only the 4.1.1 was reported in the earlier survey.[8] The recovery of different isomers serves to highlight the difficulty in mapping the complex landscape of the potential energy surface underlying microhydration. The optimized geometries for the six isomers found in our search are given in Table SI of the supplementary material,[38] and their energies are listed in Table I.

One key feature of all the structures found in this work (as well as those in Ref. 8) is that the free hydrogen atoms are rotated away from the Cs^+ center. Note that, unlike the situation in the hydration of divalent metal ions, where non-interacting water molecules build up the first solvent shell,[39–41] the weaker Cs^+-water interaction apparently allows partial formation of a H-bonded network leading to an asymmetrical solvation scenario akin to that at play in anion hydrates.[1,42,43] The resulting structures thus reflect the delicate balance between the ion-water and water-water interactions.

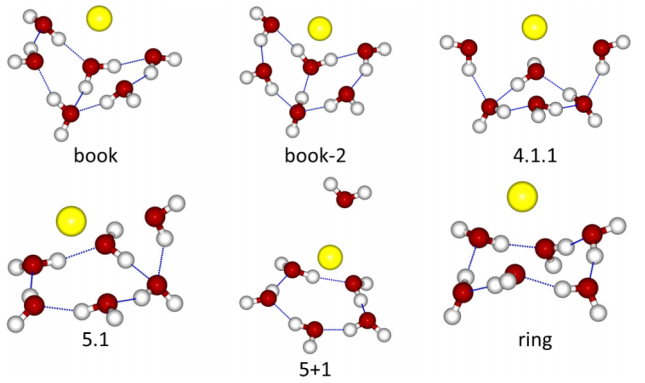

FIG. 2. Structures of the six lowest energy isomers of the $Cs^+(H_2O)_6$ cation optimized at the MP2/aug-cc-pVDZ level of theory, obtained with an effective core potential (ECP) for Cs developed by Ross *et al.*[36] Of those geometries, only the 4.1.1 has been reported earlier by Lisy and coworkers.[8] Energy differences between geometries are given in Table I, with the 4.1.1 being the lowest after zero-point correction.

The global minimum energy structure at the MP2/ADZ level is the book isomer (Fig. 2), with the book-2 structure lying 0.54 kcal/mol higher and the 4.1.1 isomer, which Lisy and co-workers reported as the global minimum,[8] located 0.05 kcal/mol above book-2. The other isomers are significantly higher in energy (>0.97 kcal/mol) relative to the book isomer. Correcting for ZPE at the harmonic level, however, brings the 4.1.1 isomer lowest (see Table I), with the book and 5.1 isomers now 0.18 and 0.27 kcal/mol, respectively, above it. To assess the robustness of this energy ordering, we have also performed calculations that include the Gibb's free energy present at room temperature (298.15 K). Inclusion of this effect further stabilizes the 4.1.1 isomer over the book by about 1 kcal/mol.

Because two of the isomers (book and 4.1.1) lie so close in energy that their relative energies depend on the inclusion of ZPE, we appeal to the experimental IR spectrum to establish which of these two (or both) is created in the low temperature ion source (see experimental details in Section II). The CIVP spectrum of the cryogenically cooled (~30 K), D_2-tagged $Cs^+(H_2O)_6$ cluster is presented in Fig. 3(b). This relatively simple spectrum consists of three main features (IHB_α, IHB_β, and F), each with multiplet structure, including a distinct doublet in the free OH stretching region near 3700 cm^{-1} (F). The locations of the free OH stretches of a water molecule in the $Cs^+(H_2O)$ binary cluster, in which both OH groups are non-bonded (3635 and 3712 cm^{-1}),[44] are also indicated by arrows in Fig. 3(b). The band lowest in energy at 3443 cm^{-1} (IHB_α) clearly results from inter-water H-bonding and is also the broadest, with hints of partially resolved structure on both the high and low energy shoulders of the main feature. The sharp absorption between these two near 3550 cm^{-1} (IHB_β) falls below the free OH region and therefore suggests the presence of a second, weaker donor H-bond in the network.

Unfortunately, both the book and 4.1.1 isomers (structure insets in Fig. 3) match the criteria imposed by this empirical analysis of the pattern, and thus we cannot make a definitive assignment by inspection. We therefore turn to the computed infrared spectra, obtained at the CCSD(T)/ADZ level to circumvent the systematic overestimation of the OH bond distance and corresponding red-shifts of the harmonic frequencies at the commonly used MP2 level.[52] The coupled

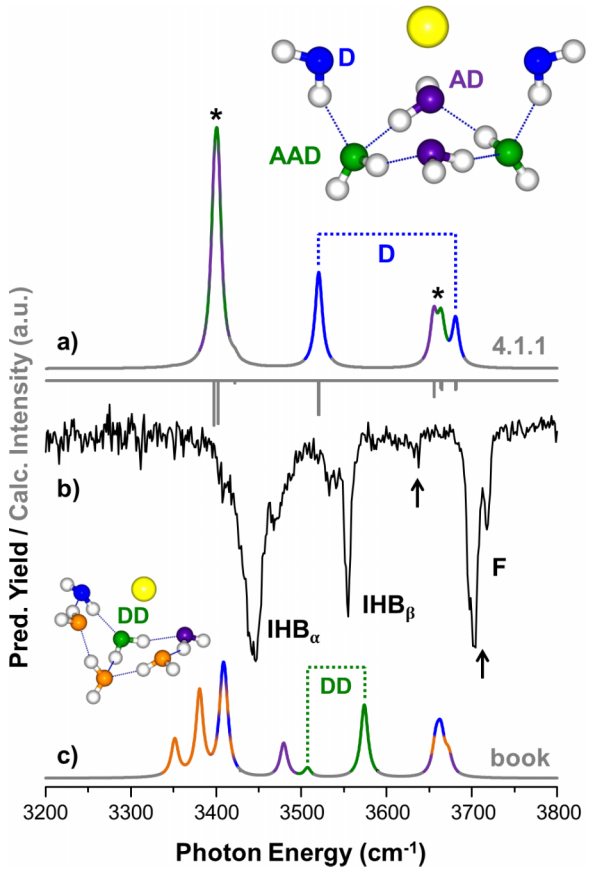

FIG. 3. Comparison of calculated spectra for the 4.1.1 Cs^+ hexahydrate isomer at the CCSD(T) level of theory, including anharmonic effects according to Eq. (1) in the top trace (a) with the book isomer at the same level in the lower trace (c). The experimental spectrum obtained by D_2 tagging in trace (b) is entirely reproduced by the predictions for the 4.1.1 structure displayed in the insert. The free OH symmetric and asymmetric stretch of the non-hydrogen bonded water molecules in the $Cs^+(H_2O)$ complex are indicated by the arrows and distinguishable water molecules in each isomer are color-coded by the oxygen atom, D (blue), AD (purple), and AAD (green). The H_2O molecule adopting an ADD configuration in the book isomer and its resulting IR bands are also indicated in green. The closely spaced doublets in (a), denoted (*), originate from the AD and AAD sites, which is more apparent in the inverted stick spectrum in (a).

TABLE I. Minimum energies (E_e, a.u.) for the different low-lying $Cs^+(H_2O)_6$ isomers at the MP2/ADZ level of theory, including zero-point corrections (ZPE, kcal/mol), total energies E_0 (kcal/mol), and relative energies ΔE_e and ΔE_0 (kcal/mol).

Isomer	E_e	ZPE[a]	ΔE_e[b]	E_0[c]	ΔE_0[d]
Book	−477.550 247 88	94.310	0.00	94.310	0.18
Book-2	−477.549 383 05	94.486	0.54	95.029	0.90
4.1.1	−477.549 308 03	93.539	0.59	94.129	0.00
5.1	−477.548 701 15	93.427	0.97	94.398	0.27
Ring	−477.544 742 29	93.544	3.45	96.999	2.87
5 + 1	−477.543 699 58	92.038	4.11	96.147	2.02

[a] $ZPE = \frac{1}{2}\Sigma_k \hbar\omega_k$.
[b] $\Delta E_e = E_e - E_e(\text{book})$.
[c] $E_0 = \Delta E_e + ZPE$.
[d] $\Delta E_0 = E_0 - E_0(4.1.1)$.

cluster harmonic frequencies were obtained employing the Z-matrix formulation, which considerably reduces the number of single point energy calculations needed to numerically evaluate the second derivatives (1328 and 2653 for the 4.1.1 and book isomers, respectively).[45] Another challenge is to account for mechanical anharmonicities common to H-bonded systems[46–48] at the coupled cluster level. Given the limitations of computational resources, this information is not accessible through a straightforward approach. We therefore calculated the 3rd and 4th order potential energy derivatives at the MP2/ADZ optimal geometry, as implemented in Gaussian09,[49] and used them to estimate the vibrational anharmonic frequencies. The MP2/ADZ anharmonicities, calculated as the difference between the anharmonic and harmonic frequencies, were then used to correct the CCSD(T)/ADZ harmonic frequencies for anharmonic effects. A second term was added to account for errors due to basis set limitations, as it corrects the "anharmonic" CCSD(T)/ADZ frequencies for the difference between double (ADZ) and triple ξ (ATZ) at the MP2 level. Overall, this method can be summarized as follows:

$$\upsilon_{\mathrm{CCSD(T)/ATZ}} \approx \omega_{\mathrm{CCSD(T)/ADZ}} + (\upsilon_{\mathrm{MP2/ADZ}} - \omega_{\mathrm{MP2/ADZ}}) + (\omega_{\mathrm{MP2/ATZ}} - \omega_{\mathrm{MP2/ADZ}}), \quad (1)$$

where ω and υ are the predicted harmonic and anharmonic (VPT2) frequencies,[50,51] each using the basis set in their respective indices. The previous application of Eq. (1) for neutral water clusters up to the hexamer[52] suggests that the correction due to anharmonicity (first term in parentheses) amounts to ~200 cm^{-1}, whereas the shifts due to the size of the basis set (second term in parentheses) are much smaller (<20 cm^{-1}).

Using this procedure, we obtained the unscaled vibrational spectra of the 4.1.1 and book clusters displayed in Figs. 3(a) and 3(c), respectively. Comparison with the experimental data in trace (b) indicates that the cluster unambiguously adopts the 4.1.1 structure. The accuracy with which this formalism reproduces the observed band positions without relying on the usual scaling factors is worth special emphasis and further details on Eq. (1) are described in the supplementary material.[38]

Of course, the correction described by Eq. (1) is confined to fundamentals, and although compelling, there is a possibility that anharmonic coupling between vibrational modes could compromise this agreement between theory and experiment. To provide a much more definitive structural assignment, we next exploit an experimental procedure that can verify assignments of bands to motions of the three structurally distinct water molecules in the H-bonded arrangement (D, AD, and AAD colored blue, purple, and green, respectively, in the 4.1.1 structure at the top of Fig. 3, where A and D denote hydrogen bond acceptor and donor, respectively). For example, the computed spectrum in Fig. 3(a) is color-coded to indicate the dominant contributions from the H-bond single donor (blue) site, which should contribute both to the highest energy shoulder on the free OH doublet and the intermediate band (IHB_β) near 3550 cm^{-1}. On the other hand, in the assignment scheme predicted for the book isomer, the IHB_β feature originates from a double donor network site (DD), which yields the two bands bracketed in green in Fig. 3(c). These differences in the embedded correlation between the two OH oscillators (blue and green brackets in Fig. 3) should be readily apparent using isotopomer-selective spectroscopy of the $Cs^+(D_2O)_5H_2O$ cluster with an intact H_2O molecule.

B. Isotopic labeling of a single intact water molecule in the ionic cluster assembly

We first establish the structural integrity of the H_2O molecule in the putative $Cs^+(D_2O)_5(H_2O)$ isotopologue by inspection of the observed pattern of bands in the intramolecular bending region from 1100 to 1700 cm^{-1}. The three band origins associated with the three isotopologues (D_2O, HDO, and H_2O) lie sufficiently far apart (arrows in Fig. 4(c)) that any significant contribution from HDO would be readily apparent. The spectrum of the $Cs^+(D_2O)_5(H_2O)$ ion packet is shown in Fig. 4(c), and it displays only two isolated transitions at 1180 and 1610 cm^{-1} corresponding to the D_2O and H_2O bending modes, respectively. The suppression of H/D intramolecular exchange evident by this spectroscopic measurement indicates that it does not occur at the elevated (300 K) temperature regime where H_2O condensation takes place. Note that the kinetic upper bound set by this behavior

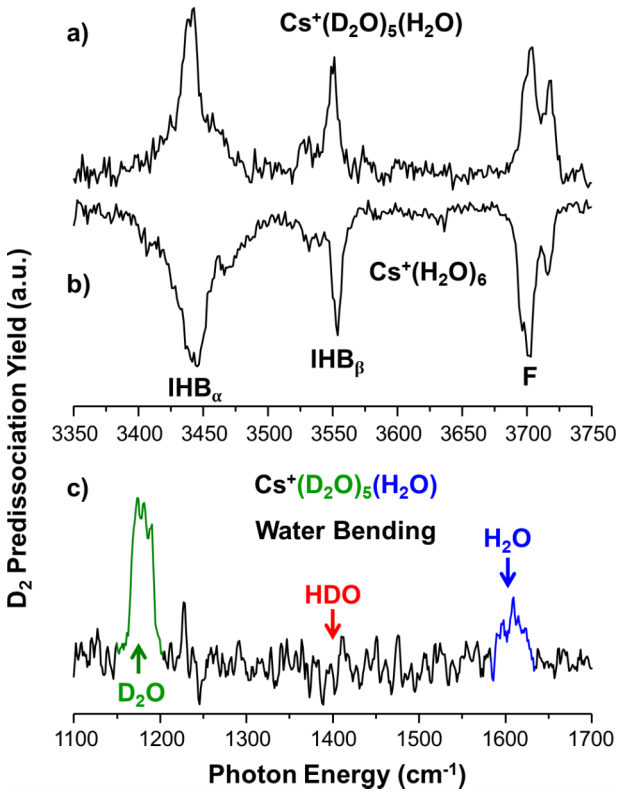

FIG. 4. Comparison of the CIVP spectra of D_2-tagged $Cs^+(D_2O)_5(H_2O)$ (a) and $Cs^+(H_2O)_6$ clusters (b). The very subtle changes in the OH stretching region, in conjunction with the absence of a HDO bending transition in the $Cs^+(D_2O)_5(H_2O)$ spectrum (red arrow, trace c), establish the experimental proof for the suppression of proton scrambling, e.g., formation of HDO. The position of the isolated bending motions of D_2O, HDO, and H_2O are indicated by arrows in (c).

includes the drift time of about 300 μs from the exchange region to the entrance to the cold trap.

Fig. 4 also compares the $Cs^+(H_2O)_6$ spectrum with that of the isotopically labeled $Cs^+(D_2O)_5(H_2O)$ cluster in traces 4(b) and 4(a), respectively. Interestingly, these spectra are nearly identical! First, this implies that the labeled molecule indeed occupies all distinct sites with roughly equal probability. More importantly, the fact that the $Cs^+(H_2O)_6$ spectrum is reproduced by the mixed isotopologue verifies that the band locations are established by the properties of a single molecule in a particular site (as opposed to being delocalized, for example, through strong coupling between sites). This observation is key to the isotopomer-selective approach in identifying the spectral signatures of these sites within a homogeneous ensemble.

C. Spectral isolation of the vibrational signatures of the intact H_2O molecule

Since the labeled water molecule occupies all available sites, the spectrum in Fig. 4(a) must be a heterogeneous convolution of many distinct spectra arising from each isotopomer. To isolate the spectra of each distinct species, we exploit the two-color IR-IR hole-burning scheme (IR^2 MS^3) described in detail earlier.[13,14] In this method, a probe laser is placed on a particular transition in the spectrum while a powerful pump laser is scanned upstream of the probe region to remove population at each resonance. When the scanned laser excites a transition common to the isotopomer monitored by the probe laser, a dip is registered in the probe signal, thus revealing all bands associated with the probed isotopomer.[12]

The application of this method to the $Cs^+(D_2O)_5(H_2O)$ isotopomers is presented in Fig. 5. The lower panel (c) corresponds to the "dip" spectrum obtained when the probe laser is tuned to the highest energy shoulder on the free OH (F_β). This necessarily results in a dip when the pump laser is scanned through this feature. The second strong dip occurs at the key IHB_β 3550 cm^{-1} band, immediately verifying the assignment of structure to the 4.1.1 isomer. Setting the probe on the lower energy 3699 cm^{-1} feature (F_α) then results in the dip spectrum displayed in Fig. 5(b). The two features associated with the D-type water molecules (blue) are absent, while two strong dips again appear. One of these appears at probe frequency and the other at the lowest energy IHB_α band centered at 3443 cm^{-1}. These are correctly predicted to arise from the H-bonded OH groups (IHB_α) involved in the four water molecules forming the homodromic tetramer at the base of the 4.1.1 assembly. Sample experimental traces signaling the correlation of two IR transitions are shown in the supplementary material.[38] Unfortunately, the predicted splitting of the tetramer water bands (AD and AAD) due to the increased acidity of the two water molecules accepting two H-bonds from the flanking D-type waters (blue) was not clearly observed, although both the dip features associated with the 3699 cm^{-1} probe transition (F_α) are broader than those arising from the D-type water molecules (blue), consistent with an unresolved doublet.

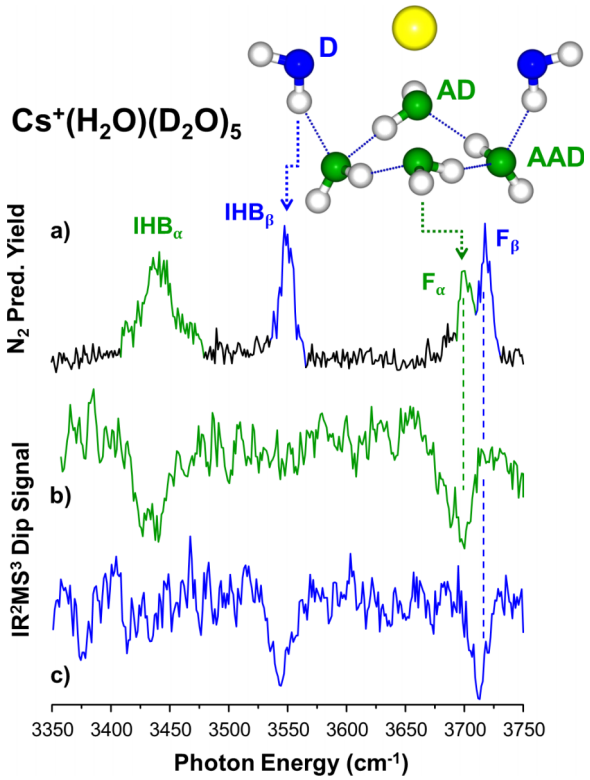

FIG. 5. Trace (a) represents the CIVP spectrum of N_2-tagged $Cs^+(D_2O)_5(H_2O)$, with the mayor feature labeled in agreement with the text. The two traces in the bottom ((a) and (b)) correspond to the IR^2MS^3 spectra when the probe frequency is tuned in resonance with the free OH stretches, F_α or F_β, respectively. This scheme yields the IR spectrum of the single H_2O molecule in the green and blue sites indicated in the top structure inset.

D. Effects of the internal electric fields in the $Cs^+(H_2O)_6$ cluster on its vibrational spectrum

The reconstruction of the IR spectrum from the behavior of the individual water "building blocks" is interesting, naturally raising the question of what properties of the binding sites lead to the locations of the two OH stretches. In the theoretical treatment of the IR spectrum of liquid water, these frequencies are often traced to the local electric field imposed onto each H_2O by the surrounding water molecules.[53–64] The central concept in the application to liquid-phase spectra is the use of a particular vibrational mode as an antenna to probe the *effective* electric field fluctuations due to its surrounding environment. Early work in this area employed continuum descriptions of electrostatics,[53–55] while more recent work utilized electric fields arising from classical point charges.[57–63] The cold cluster regime provides an excellent medium in which to explore these ideas when the particular sites giving rise to relatively sharp (i.e., persistent rather than fluctuating) vibrational features are known.

We will explore the electric fields arising from quantum mechanical charge distributions for the $Cs^+(H_2O)_6$ cluster. Is it important to emphasize that this approach is distinct from previous studies in that we calculate the electric field coupling to vibrational shifts from an *ab initio* perspective. This yields more "exact" results in the absolute sense as there is much uncertainty from continuum, point charges, or polarizable sources. Specifically, the electric fields on the

hydrogen atom sites are calculated as those arising from the quantum mechanical charge densities of all the other atoms in the system excluding only those atoms with the water molecule for which the field is being evaluated. These electric fields are then projected onto the OH bond vectors corresponding to each vibrational antenna and it is in this sense that they must be considered as *effective* arising from the surrounding atoms.

To be consistent with the previous work by Skinner *et al.*,[59,65,66] we define the hydrogen nuclei as the probe location and all other atoms of the solvation network as the source of the electric field. Subsequently, we match the projected electric fields to reproduce the observed IR spectrum within the formalism of vibrational Stark spectroscopy, where the frequency shifts are induced by the electric fields within the system (i.e., vibrational solvatochromism or internal vibrational Stark spectroscopy) as opposed to vibrational shifts induced in the system by an externally applied electric field (i.e., vibrational electrochromism or external Stark spectroscopy). The fundamental relationship between frequency shifts $\Delta\omega$ and projected electric field E_{proj} used in 2nd order vibrational Stark spectroscopy is given by

$$\begin{aligned}\Delta\omega\left(E_{proj}\right) &= \omega(E_{proj}) - \omega(0)\\ &= -\Delta\mu \cdot E_{proj} - \frac{1}{2}E_{proj} \cdot \Delta\alpha \cdot E_{proj}, \qquad (2)\end{aligned}$$

where $\Delta\mu$ is the "Stark tuning rate" or effective difference dipole moment, and $\Delta\alpha$ is the effective difference polarizabilities between ground and excited states. As pointed out by Reimers and Hush,[56] $\Delta\mu$ and $\Delta\alpha$ are not the exact changes in the expectation values of the dipole and polarizability operators induced by a vibrational transition, however, we retain the notation and language to be consistent with the vibrational Stark spectroscopy literature.

In order to evaluate the electric field at the twelve hydrogen sites in the $Cs^+(H_2O)_6$ cluster, each probe water molecule was removed, in turn, from the quantum mechanical calculation (MP2/ADZ) and the resulting electric potential was generated on a computational grid, which was then numerically differentiated to obtain the electric field at the probe molecule's hydrogen sites. The total electric field $\hat{E}$ was then projected onto the OH bond vector $\hat{u}_{OH}$ at an angle θ, resulting in the projected electric field E_{proj}. Fig. 6(a) displays the $Cs^+(H_2O)_6$ H-indices, and the corresponding projected electric fields E_{proj} are graphed in the lower panel 6(b). As expected from the cluster geometry, six OH groups are free (green background) and six are engaged in H-bond formation (blue).

It is important to recognize that the strength of the *ab initio* electric fields are larger than those applied in vibrational Stark spectroscopy. Interestingly, the *ab initio* electric fields are quantitatively comparable to the electric field distributions found within pure SPC/E water,[67,68] ranging from 50 to 400 MV/cm, with an average field peaked at 200 MV/cm and a FWHM of about 160 MV/cm.

Now we consider the internal Stark vibrational shifts (solvatochromic) of the OH groups in the 4.1.1 structure. Using the projected electric field E_{proj} for the three OH groups corresponding to the three main spectral features with frequencies $\omega(E_{proj})$, the electric field mapping according to Eq. (2) yields the following fit parameters: $\omega(0)$ = 3837.8 cm^{-1}, $\Delta\mu$ = 2.0426 cm^{-1}/(MV/cm), and $\Delta\alpha/2$ = −0.000 959 7 cm^{-1}/(MV/cm)^2 using Cramer's rule.[69] This is consistent with the work of Skinner *et al.* who obtained a linear $\Delta\mu$ = 2.1 cm^{-1}/(MV/cm),[70] neglecting quadratic terms, and $\Delta\mu$ = 0.98 cm^{-1}/(MV/cm)[65] with $\Delta\alpha/2$ = 0.000 326 cm^{-1}/(MV/cm)^2 upon their inclusion for SPC/E

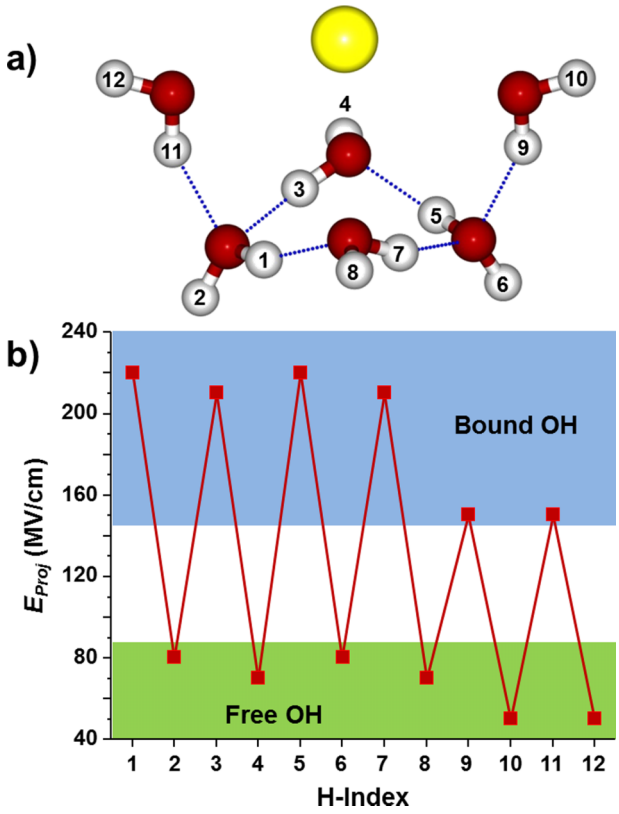

FIG. 6. (a) Optimized geometry (CCSD(T)/ADZ) and H-indices for the $Cs^+(H_2O)_6$ cluster. (b) Plot of the projected E_{proj} fields. Blue/black backgrounds denote the set of six H-atoms that are hydrogen bonded/free, respectively.

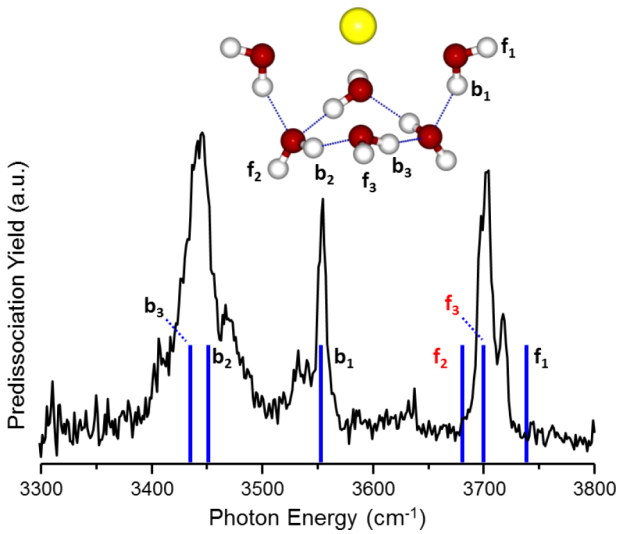

FIG. 7. Plots of the experimental spectra (black) and the quadratic field-to-frequency mapping (blue) for $Cs^+(H_2O)_6$. The f and b notation denotes free and bound OH groups. Red labels indicate a switch in band ordering relative to the CCSD(T)/ATZ predictions.

water clusters simulated at ambient temperature. The results for the electric field-to-frequency mapping are presented in Fig. 7, where the symbols f_x and b_y denote free and bound OH groups, respectively, and the indices correspond to bond displacements of the OH groups indicated in the top structure inset. The mapped spectrum (blue sticks) accurately accounts for the observed bands (black curve), yet fails to recover the observed multiplet character of certain features. In particular, f_2 and f_3 and b_2 and b_3 (labeled red in Fig. 7) are switched relative to the CCSD(T)/ATZ anharmonic assignments that were made using the amplitudes of the normal modes. Future *ab initio* studies of the projected electric fields will incorporate thermal sampling to include relevant configurations beyond the global energetic minimum to investigate their influence on the lineshapes, positions, and mode assignments. Unfortunately, there are no experimental Stark tuning rates for this cluster, thus our results stand as a prediction for the future; however, some recent measurements and calculations have been performed on vitrified water.[71]

IV. SUMMARY

This study reports several comprehensive improvements leading to the understanding and correct interpretation of the effects of microhydration in the prototypical $Cs^+(H_2O)_6$ cluster. These involve the accurate theoretical treatment of both the relative energy ordering of the different networks present in the various low-lying isomers and the spectral features of the water in the first solvation shell at the coupled cluster level. A further addition to incorporate the anharmonic coupling terms at the MP2 level was shown to yield excellent agreement with the OH stretching transitions observed with CIVP spectroscopy. To validate the assignments of spectral features to site specific water molecules within the network, we use IR-IR isomer specific double resonance techniques. This approach isolates the contributions of two distinct sites within the cluster, and unambiguously allows assignment of the experimentally prepared cluster to the 4.1.1 form based on a water tetramer with two flanking water molecules. Taken together, this complementary experiment-theory approach confirms that it is the MP2 harmonic frequencies that need to be corrected at the more accurate CCSD(T) level. The assignment of the 4.1.1 isomer as the global minimum of the $Cs^+(H_2O)_6$ cluster is also consistent with the finding that it is the lowest energy isomer when corrections for the (anharmonic) zero-point energy are taken into account.

ACKNOWLEDGMENTS

M.A.J. would like to thank the U.S. National Science Foundation (NSF) under Grant No. CHE-1465100. E.M., S.M.K., and S.S.X. were supported by the U.S. Department of Energy, Office of Science, Office of Basic Energy Sciences, Division of Chemical Sciences, Geosciences and Biosciences. Pacific Northwest National Laboratory (PNNL) is a multiprogram national laboratory operated for DOE by Battelle. This research also used resources of the National Energy Research Scientific Computing Center, which is supported by the Office of Science of the U.S. Department of Energy under Contract No. DE-AC02-05CH11231.

[1]W. H. Robertson and M. A. Johnson, Annu. Rev. Phys. Chem. **54**, 173–213 (2003).
[2]C. T. Wolke, F. S. Menges, N. Totsch, O. Gorlova, J. A. Fournier, G. H. Weddle, M. A. Johnson, N. Heine, T. K. Esser, H. Knorke, K. R. Asmis, A. B. McCoy, D. J. Arismendi-Arrieta, R. Prosmiti, and F. Paesani, J. Phys. Chem. A **119**, 1859–1866 (2015).
[3]C. A. Wick and S. S. Xantheas, J. Phys. Chem. B **113**, 4141–4146 (2009).
[4]S. S. Xantheas, Can. J. Chem. Eng. **90**, 843–851 (2012).
[5]A. B. Wolk, C. M. Leavitt, E. Garand, and M. A. Johnson, Acc. Chem. Res. **47**, 202–210 (2014).
[6]P. D. Carnegie, A. B. McCoy, and M. A. Duncan, J. Phys. Chem. A **113**, 4849–4854 (2009).
[7]A. B. McCoy, T. L. Guasco, C. M. Leavitt, S. G. Olesen, and M. A. Johnson, Phys. Chem. Chem. Phys. **14**, 7205–7214 (2012).
[8]M. Kolaski, H. M. Lee, Y. C. Choi, K. S. Kim, P. Tarakeshwar, D. J. Miller, and J. M. Lisy, J. Chem. Phys. **126**, 074302 (2007).
[9]H. Ke, C. van der Linde, and J. M. Lisy, J. Phys. Chem. A **118**, 1363–1373 (2014).
[10]C. J. Weinheimer and J. M. Lisy, J. Chem. Phys. **105**, 2938–2941 (1996).
[11]J. A. Fournier, C. T. Wolke, C. J. Johnson, M. A. Johnson, N. Heine, S. Gewinner, W. Schollkopf, T. K. Esser, M. R. Fagiani, H. Knorke, and K. R. Asmis, Proc. Natl. Acad. Sci. U. S. A. **111**, 18132–18137 (2014).
[12]T. L. Guasco, B. M. Elliott, M. A. Johnson, J. Ding, and K. D. Jordan, J. Phys. Chem. Lett. **1**, 2396–2401 (2010).
[13]R. A. Relph, T. L. Guasco, B. M. Elliott, M. Z. Kamrath, A. B. McCoy, R. P. Steele, D. P. Schofield, K. D. Jordan, A. A. Viggiano, E. E. Ferguson, and M. A. Johnson, Science **327**, 308–312 (2010).
[14]B. M. Elliott, R. A. Relph, J. R. Roscioli, J. C. Bopp, G. H. Gardenier, T. L. Guasco, and M. A. Johnson, J. Chem. Phys. **129**, 094303 (2008).
[15]V. Buch, T. Tarbuck, G. L. Richmond, H. Groenzin, I. Li, and M. J. Shultz, J. Chem. Phys. **127**, 204710 (2007).
[16]D. S. Walker and G. L. Richmond, J. Phys. Chem. C **111**, 8321–8330 (2007).
[17]S. T. Roberts, P. B. Petersen, K. Ramasesha, A. Tokmakoff, I. S. Ufimtsev, and T. J. Martinez, Proc. Natl. Acad. Sci. U. S. A. **106**, 15154–15159 (2009).
[18]E. H. G. Backus and M. Bonn, J. Chem. Phys. **121**, 1038–1049 (2004).
[19]M. Smits, A. Ghosh, M. Sterrer, M. Muller, and M. Bonn, Phys. Rev. Lett. **98**, 098302 (2007).
[20]O. Isaienko and E. Borguet, Opt. Express **20**, 547–561 (2012).
[21]S. Dewan, V. Carnevale, A. Bankura, A. Eftekhari-Bafrooei, G. Fiorin, M. L. Klein, and E. Borguet, Langmuir **30**, 8056–8065 (2014).
[22]M. J. Ryding, A. S. Zatula, P. U. Andersson, and E. Uggerud, Phys. Chem. Chem. Phys. **13**, 1356–1367 (2011).
[23]A. S. Zatula, M. J. Ryding, P. U. Andersson, and E. Uggerud, Int. J. Mass Spectrom. **330**, 191–199 (2012).
[24]M. Z. Kamrath, E. Garand, P. A. Jordan, C. M. Leavitt, A. B. Wolk, M. J. Van Stipdonk, S. J. Miller, and M. A. Johnson, J. Am. Chem. Soc. **133**, 6440–6448 (2011).
[25]P. J. Kelleher, C. J. Johnson, J. A. Fournier, M. A. Johnson, and A. B. McCoy, J. Phys. Chem. A **119**, 4170–4176 (2015).
[26]X. B. Wang and L. S. Wang, Rev. Sci. Instrum. **79**, 073108 (2008).
[27]X. B. Wang, H. K. Woo, and L. S. Wang, J. Chem. Phys. **123**, 051106 (2005).
[28]M. A. Johnson and W. C. Lineberger, in *Techniques for the Study of Ion-Molecule Reactions*, edited by J. M. Farrar and W. H. Saunders, Jr. (Wiley, New York, 1988), p. 591.
[29]M. Z. Kamrath, R. A. Relph, T. L. Guasco, C. M. Leavitt, and M. A. Johnson, Int. J. Mass Spectrom. **300**, 91–98 (2011).
[30]C. van der Linde and M. K. Beyer, J. Phys. Chem. A **116**, 10676–10682 (2012).
[31]C. van der Linde and M. K. Beyer, Phys. Chem. Chem. Phys. **13**, 6776–6778 (2011).
[32]Z. Sun, C. K. Siu, O. P. Balaj, M. Gruber, V. E. Bondybey, and M. K. Beyer, Angew. Chem., Int. Ed. **45**, 4027–4030 (2006).
[33]L. A. Lajohn, P. A. Christiansen, R. B. Ross, T. Atashroo, and W. C. Ermler, J. Chem. Phys. **87**, 2812–2824 (1987).
[34]T. H. Dunning, Jr., J. Chem. Phys. **90**, 1007–1023 (1989).
[35]R. A. Kendall, T. H. Dunning, Jr., and R. J. Harrison, J. Chem. Phys. **96**, 6796–6806 (1992).
[36]R. B. Ross, J. M. Powers, T. Atashroo, W. C. Ermler, L. A. Lajohn, and P. A. Christiansen, J. Chem. Phys. **93**, 6654–6670 (1990).
[37]M. Valiev, E. J. Bylaska, N. Govind, K. Kowalski, T. P. Straatsma, H. J. J. Van Dam, D. Wang, J. Nieplocha, E. Apra, T. L. Windus, and W. de Jong, Comput. Phys. Commun. **181**, 1477–1489 (2010).

[38]See supplementary material at http://dx.doi.org/10.1063/1.4941285 for further information and details about the isomer geometries and computational methods.
[39]C. J. Johnson, L. C. Dzugan, A. B. Wolk, C. M. Leavitt, J. A. Fournier, A. B. McCoy, and M. A. Johnson, J. Phys. Chem. A **118**, 7590–7597 (2014).
[40]M. F. Bush, J. T. O'Brien, J. S. Prell, C. C. Wu, R. J. Saykally, and E. R. Williams, J. Am. Chem. Soc. **131**, 13270–13277 (2009).
[41]J. T. O'Brien and E. R. Williams, J. Phys. Chem. A **112**, 5893–5901 (2008).
[42]P. Ayotte, G. H. Weddle, J. Kim, J. A. Kelley, and M. A. Johnson, J. Phys. Chem. A **103**, 443–447 (1999).
[43]J. A. Kelley, J. M. Weber, K. M. Lisle, W. H. Robertson, P. Ayotte, and M. A. Johnson, Chem. Phys. Lett. **327**, 1–6 (2000).
[44]T. D. Vaden, B. Forinash, and J. M. Lisy, J. Chem. Phys. **117**, 4628–4631 (2002).
[45]E. Miliordos and S. S. Xantheas, J. Phys. Chem. A **117**, 7019–7029 (2013).
[46]J. A. Fournier, C. J. Johnson, C. T. Wolke, G. H. Weddle, A. B. Wolk, and M. A. Johnson, Science **344**, 1009–1012 (2014).
[47]J. A. Fournier, C. T. Wolke, M. A. Johnson, T. T. Odbadrakh, K. D. Jordan, S. M. Kathmann, and S. S. Xantheas, J. Phys. Chem. A **119**, 9425–9440 (2015).
[48]M. Torrent-Sucarrat and J. M. Anglada, J. Chem. Theory Comput. **7**, 467–472 (2011).
[49]M. J. Frisch, G. W. Trucks, H. B. Schlegel, G. E. Scuseria, M. A. Robb, J. R. Cheeseman, V. G. Zakrzewski, J. A. Montgomery, Jr., R. E. Stratmann, J. C. Burant, S. Dapprich, J. M. Millam, A. D. Daniels, K. N. Kudin, M. C. Strain, O. Farkas, J. Tomasi, V. Barone, M. Cossi, R. Cammi, B. Mennucci, C. Pomelli, C. Adamo, S. Clifford, J. Ochterski, G. A. Petersson, P. Y. Ayala, Q. Cui, K. Morokuma, P. Salvador, J. J. Dannenberg, D. K. Malick, A. D. Rabuck, K. Raghavachari, J. B. Foresman, J. Cioslowski, J. V. Ortiz, A. G. Baboul, B. B. Stefanov, G. Liu, A. Liashenko, P. Piskorz, I. Komaromi, R. Gomperts, R. L. Martin, D. J. Fox, T. Keith, M. A. Al-Laham, C. Y. Peng, A. Nanayakkara, M. Challacombe, P. M. W. Gill, B. Johnson, W. Chen, M. W. Wong, J. L. Andres, C. Gonzalez, M. Head-Gordon, E. S. Replogle, and J. A. Pople, Gaussian 98 (Revision A.1x), Gaussian Inc., Pittsburgh PA, 2001.
[50]V. Barone, J. Chem. Phys. **101**, 10666–10676 (1994).
[51]V. Barone, C. Adamo, and C. Minichino, J. Mol. Struct.: THEOCHEM **330**, 325–333 (1995).
[52]E. Miliordos, E. Apra, and S. S. Xantheas, J. Chem. Phys. **139**, 114302 (2013).
[53]L. Onsager, J. Am. Chem. Soc. **58**, 1486–1493 (1936).
[54]J. R. Platt, J. Chem. Phys. **34**, 862 (1961).
[55]W. Liptay, Angew. Chem., Int. Ed. **8**, 177 (1969).
[56]N. S. Hush and J. R. Reimers, J. Phys. Chem. **99**, 15798–15805 (1995).
[57]S. D. Fried and S. G. Boxer, Acc. Chem. Res. **48**, 998–1006 (2015).
[58]H. Lee, G. Lee, J. Jeon, and M. Cho, J. Phys. Chem. A **116**, 347–357 (2012).
[59]J. R. Schmidt, S. T. Roberts, J. J. Loparo, A. Tokmakoff, M. D. Fayer, and J. L. Skinner, Chem. Phys. **341**, 143–157 (2007).
[60]J. D. Smith, R. J. Saykally, and P. L. Geissler, J. Am. Chem. Soc. **129**, 13847–13856 (2007).
[61]J. D. Eaves, A. Tokmakoff, and P. L. Geissler, J. Phys. Chem. A **109**, 9424–9436 (2005).
[62]B. Reischl, J. Kofinger, and C. Dellago, Mol. Phys. **107**, 495–502 (2009).
[63]P. L. Geissler, C. Dellago, D. Chandler, J. Hutter, and M. Parrinello, Science **291**, 2121–2124 (2001).
[64]P. Geissinger, in *Anisotropic Organic Materials*, edited by R. Glaser and P. Kaszynski (American Chemical Society, 2009), pp. 16–32.
[65]B. Auer, R. Kumar, J. R. Schmidt, and J. L. Skinner, Proc. Natl. Acad. Sci. U. S. A. **104**, 14215–14220 (2007).
[66]S. A. Corcelli and J. L. Skinner, J. Phys. Chem. A **109**, 6154–6165 (2005).
[67]B. Sellner and S. M. Kathmann, J. Chem. Phys. **141**, 18C534 (2014).
[68]B. Sellner, M. Valiev, and S. M. Kathmann, J. Phys. Chem. B **117**, 10869–10882 (2013).
[69]G. Cramer, *Introduction à L'analyse des Lignes Courbes Algèbriques* (Frères Cramer, Genève, 1750).
[70]S. A. Corcelli, C. P. Lawrence, and J. L. Skinner, J. Chem. Phys. **120**, 8107–8117 (2004).
[71]S. Shin, H. Kang, D. Cho, J. Y. Lee, and H. Kang, J. Phys. Chem. C **119**, 15596–15603 (2015).